



Piezoelectric and elastic properties of relaxor-like PZT:Ba ceramics

Iwona Lazar¹ · Małgorzata Adamczyk-Habrajska² · Marian Pawełczyk³ · Michał Górny¹ · Anna Zawada⁴ · Krystian Roleder¹

Received: 10 October 2017 / Accepted: 13 February 2018 / Published online: 20 February 2018

© The Author(s) 2018. This article is an open access publication

Abstract

The solid solutions of $\text{PbZr}_{1-x}\text{Ti}_x\text{O}_3$ (PZT) are the most known and widely applicable piezoelectric ceramic materials. The influence of different dopants on PZT properties has been studied for many years. Some of such compositions have revealed a behavior typical for ferroelectric relaxors. In the case of $\text{Pb}_{0.75}\text{Ba}_{0.25}\text{Zr}_{0.70}\text{Ti}_{0.30}\text{O}_3$ ceramics (abbreviation PBZT 25/70/30), prepared by mixed-oxide processing technique elastic, it was found that macroscopic piezoelectric activity is present far above the temperature at which structural changes and maximum of permittivity occur in unpoled samples (~ 200 °C). Anomalies of the elastic and piezoelectric properties have been observed very clearly near the temperature of 152 °C. Within the temperature range of 152–220 °C, unstable piezoelectric properties have been detected due to the existence of polar micro/nano-clusters and non-trivial elastic-electric interactions between them, through the non-polar paraelectric matrix. The origin of such interactions could be lattice instabilities, dynamic change in polar cluster sizes, and fluctuations in chemical composition. Based on the results of the research, it can be said that PZT ceramics of such composition is a relaxor-like material and it is not a ferroelectric relaxor.

Keywords X-ray methods · Dielectric properties · Piezoelectric properties · Elastic properties · PZT

1 Introduction

Lead zirconate titanate $\text{PbZr}_{1-x}\text{Ti}_x\text{O}_3$ (PZT) is a perovskite type ABO_3 structured material, with well-known piezoelectric, pyroelectric and dielectric properties, widely used in practical applications. Modified by various dopants, PZT ceramics are mainly investigated for piezoelectric applications, due to their unique properties such as high response speed, high piezoelectric modules, and lower power requirements, to mention but a few of them. They have been used for fabricating nonvolatile memories, pyroelectric detectors, photoelectric devices and piezoelectric

actuators [1, 2]. The lanthanum-modified lead zirconate titanate (PLZT) system was extensively investigated, mainly for electro-optic applications [3]. In literature, reports about properties of PZT doped with Ca, Sr or Ba have also appeared [4]. Our interest has focused on the $\text{Pb}_{1-y}\text{Ba}_y\text{Zr}_{1-x}\text{Ti}_x\text{O}_3$ (PBZT) system, the investigations of which were initiated by Smolenskii et al. [5]. Ikeda's phase diagram [6] based on the structural and dielectric measurements shows that phase transitions occurring in these ceramics and their dielectric properties are strongly dependent on both the Zr/Ti ratio and the Ba contents. The mentioned phase diagram has been confirmed by exploring the dielectric properties and electric field induced strains, and reported by Li and Heartling [7]. Moreover, they have shown that some compositions demonstrate behavior typical for ferroelectric relaxors, namely a broad maximum and strong non-Debye relaxation of permittivity. Cross [8] has shown that a characteristic feature of ferroelectric relaxor materials is, for example, the absence of macroscopic polarization and optical anisotropy at temperatures below the maximum of permittivity. Recently, Mesquita et al. [9] have observed that Ba incorporation into the PZT lattice leads to a reduction in Ti displacement from the center of oxygen octahedron when Ba concentration increases. Papers describing properties of compounds belonging to the PBZT system have been published in [10–13].

✉ Iwona Lazar
iwona.lazar@us.edu.pl

¹ Institute of Physics, University of Silesia, ul. Uniwersytecka 4, 40-007 Katowice, Poland

² Institute of Technology and Mechatronics, University of Silesia, ul. Żytnia 12, 41-200 Sosnowiec, Poland

³ Institute of Information Technologies, ul. Mickiewicza 29, Katowice, Poland

⁴ Institute of Materials Science, Technical University of Technology, Al. Armii Krajowej 19, 42-200 Częstochowa, Poland

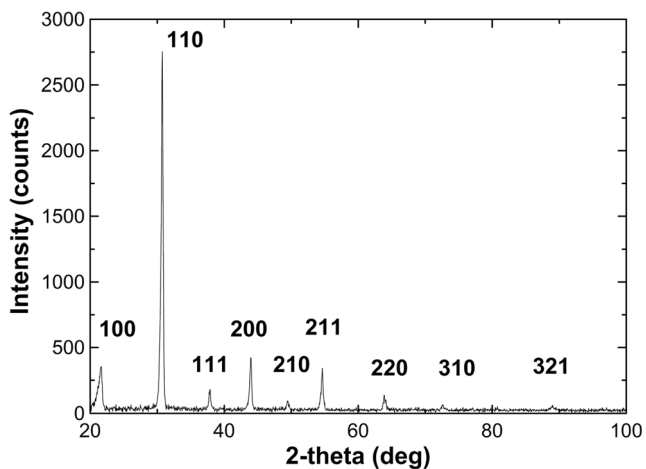
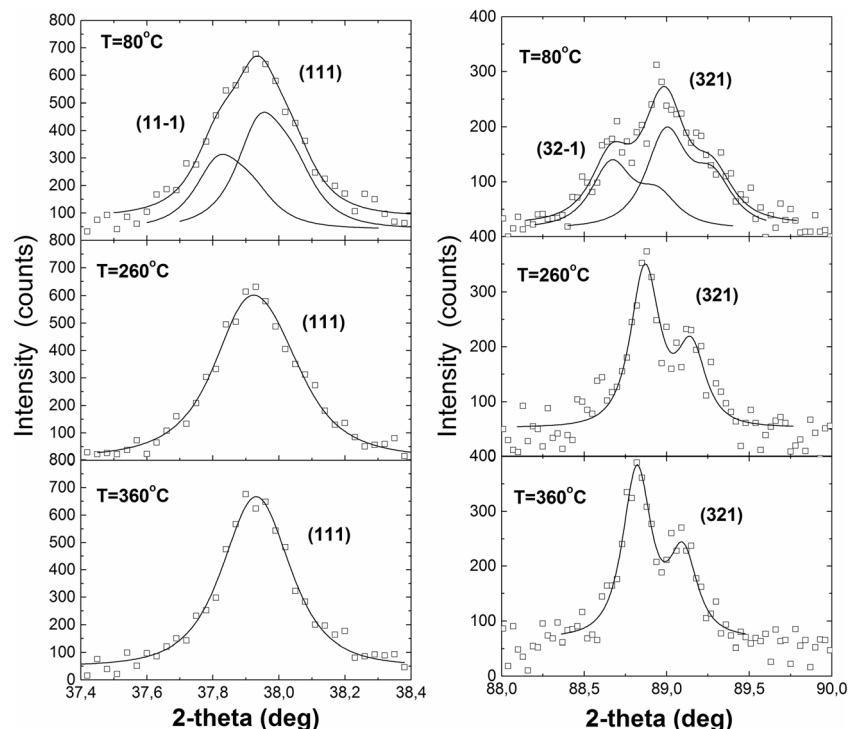


Fig. 1 XRD pattern confirming the perovskite structure of the PBZT 25/70/30 ceramics

In our earlier papers we have focused on PBZT 25/70/30 ceramics [14, 15], investigating the pyroelectric effect, thermal stimulated depolarization currents and electric conductivity. In this paper we concentrate mainly on piezoelectric properties of such ceramics. The temperature evolution of elastic coefficients and piezoelectric modulus have been determined by resonance technique. To calculate piezoelectric coefficients and the real and imaginary part of the elastic compliances, a damped forced harmonic oscillator model has been used [16, 17]. The goal was to find a correlation between the dielectric, elastic, piezoelectric and structural properties of PBZT 25/70/30 and to prove that this material does not reveal *classical* relaxor properties.

Fig. 2 Temperature evolution of (111) and (321) reflections for PBZT 25/70/30 ceramics. The spectral components $K_{\alpha 1}$ and $K_{\alpha 2}$ are visible



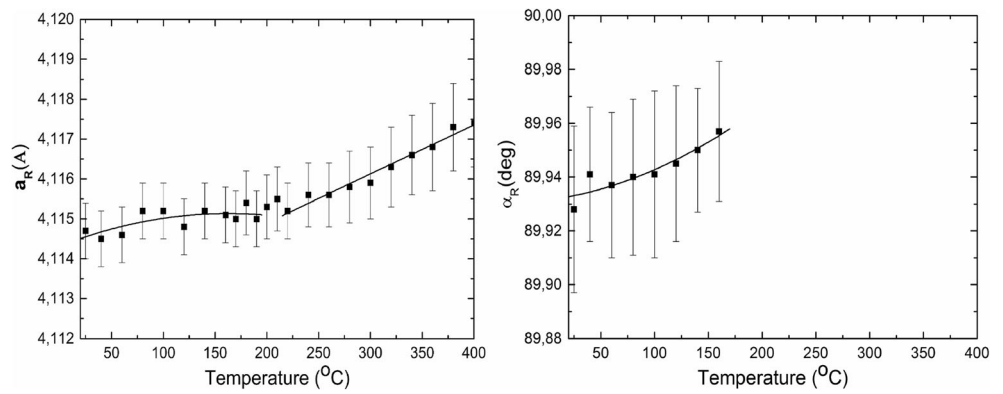
2 Material and methods

PBZT 25/70/30 ceramics have been prepared using conventional mixed-oxide processing technique. Stoichiometric amounts of the PbO, BaCO₃, ZrO₂ and TiO₂ oxides were weighted according to the formula: Pb_{0.75}Ba_{0.25}Zr_{0.70}Ti_{0.30}O₃. The thermal synthesis of the pressed mixture was carried out at 925 °C for 2 h. Then the crushed, milled and sieved materials were pressed into cylindrical pellets and again sintered at 1250 °C for 5 h. This procedure was repeated before the final sintering at 1300 °C for 7 h. The last sintering process was carried out in a double crucible with the interior atmosphere of PbO + ZrO₂, in order to preserve the predetermined composition, and in particular, to avoid the loss of PbO caused by its sublimation. The weight losses were found to be below 1%. The Archimedes displacement method with distilled water has been used to evaluate sample density that was equal to 6.8 g/cm³.

The microstructure and distribution of elements inside the grains were examined by JSM-5410 scanning electron microscope with an energy dispersive X-ray spectrometer (EDS). The accelerating voltage was equal to 15 kV and Spot Size (SS) was 55. The grain size determination was performed on a fractured surface of the ceramics.

A preliminary X-ray test was carried out at room temperature, using Huber diffractometer with θ - θ geometry, focused in Zeeman-Bohlin system, and with monochromatic CuK _{α 1} radiation. The diffraction was collected from 19° to 100° in 2 θ geometry and 0.05° steps. The XRD profiles were analysed using a software, i.e. DHN powder Diffraction System ver.

Fig. 3 Temperature changes of unit cell parameters obtained for PBZT 25/70/30 ceramics



2.3. The main x-ray tests were made in order to find out the nature of the unit cell distortion. They were performed by means of high-resolution Siemens D5000 diffractometer with θ - 2θ geometry, focused in Bragg-Brentano system, with filtered CuK_α radiation.

For piezoelectric measurements the ceramics were cut to required sample geometrical conditions of bar shape [18], with gold electrodes and having dimensions of about $4 \times 1 \times 0.5 \text{ mm}^3$. For electrical contact, thin gold wires were glued at the centre of the evaporated electrodes. The samples were poled under an external d.c. electric field of 6 kV/cm applied at 200 °C, and then slowly cooled to room temperature. The elastic compliances s_{11} , s_{33} , s_{55} , piezoelectric modulus d_{31} , d_{33} , d_{15} and electromechanical coupling factors k_{31} , k_{33} , k_{15} have been determined by resonance method. To calculate these coefficients, the forced damped harmonic oscillator model has been applied [16].

3 Results and discussion

The XRD pattern of the set of Bragg’s X-ray reflections is shown in Fig. 1. The location and intensity of nine diffraction reflections were identified. All indexes connected with the structure of perovskites were assigned. Non-perovskite reflections have not been observed. In order to determine the crystal symmetry and temperature points at which structural changes appear, the scans ($2\theta = 0.03^\circ$) of selected (111), (200), (321) Bragg’s reflections were collected in the temperature range from 25 °C to 400 °C. Structural analysis has revealed an asymmetry of X-ray reflections and hence they were treated as multiplets (see Fig. 2). The number of components, as well as the split of pseudo-regular reflection (111) into two components, and the lack of split of (200) reflections, indicate equal in size and non-perpendicular edges of unit cell. It confirms the rhombohedral symmetry reported by Mir et al. [19]. Gradual disappearance of reflections splitting above 200 °C points to transformation from rhombohedral to cubic phase. The temperature dependencies of unit cell parameters are presented in Fig. 3, in which distinct change of $a_R(T)$

dependence, as well as the angle α approaching 90° suggests structural transformation near 200 °C. Approaching 200 °C, the integral width of X-ray reflections (111) and (321) decreases, while in the case of (200) it remains unchanged (Fig. 4). This effect could be explained by a decrease in the unit cell distortion. A proof of it is the decrease of the angle between components of multiplets. Above 200 °C the reflections are well separated and the temperature dependence of their width is considerably weaker. The exception is the reflection (200) because its integral width does not change in the investigated temperature range. Moreover, this reflection is

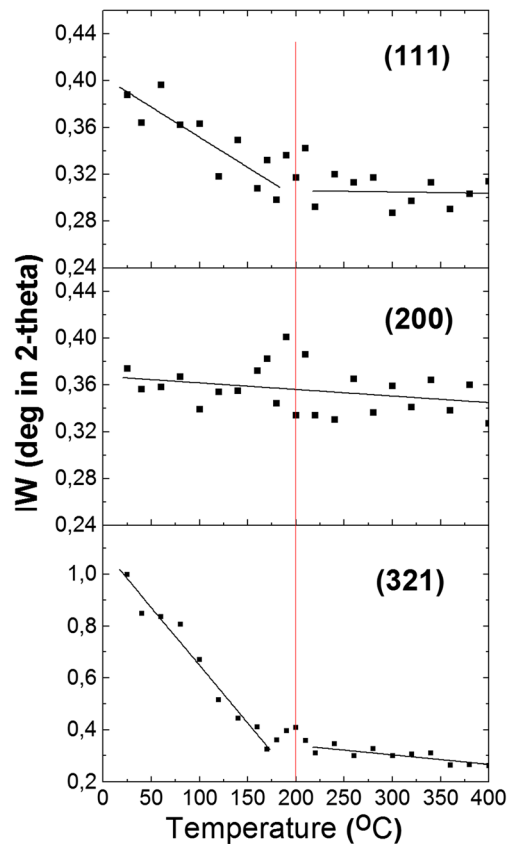


Fig. 4 Temperature dependence of integral width IW for selected X-ray reflections. Dashed line indicates the temperature of maximum permittivity (see Fig. 5)

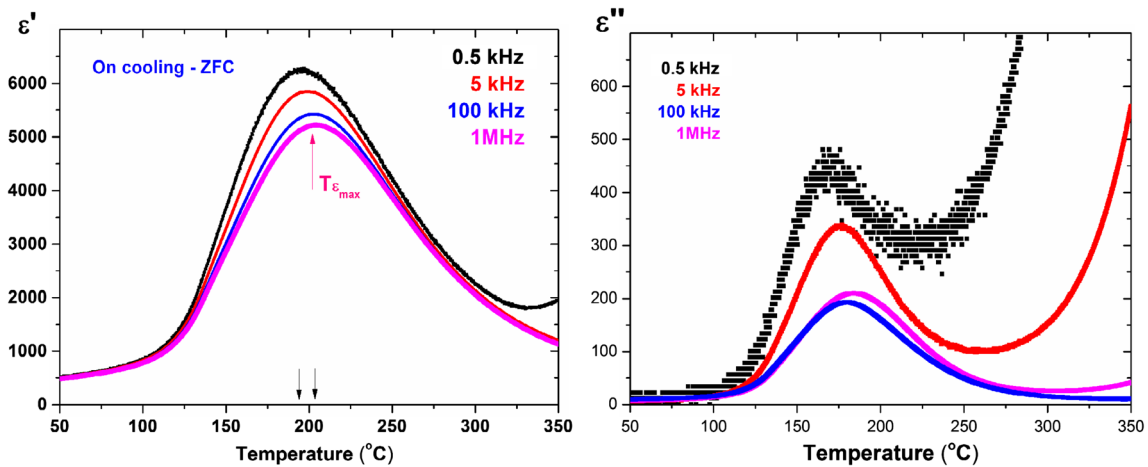


Fig. 5 Variations of zero-field cooling (ZFC) permittivity ϵ' and ϵ'' measured at chosen frequencies for unpoled PBZT 25/70/30 ceramics. Black arrows indicate a range of $T_{\epsilon_{\max}}$ changes with frequency

abnormally wide in comparison with others, and wider than (321). Similar results should be visible in the case of (100) and (400) reflections, but we were not able to observe them because the latter was asymmetrical due to equipment limitations (angle θ too small), and the former was too weak to be detected. Hence, we assume that the peculiar behavior of the (200) reflection is most probably due to structure disorder in the investigated material, as reported in the paper [14], and also confirmed in our EDS study. Of interest is the correlation between the dependence of remnant polarization reported in the paper [14] and the value of integral width IW of the reflection (200) above 200 °C, presented in Fig. 4. While the remnant polarization is not measurable above 200 °C, relatively high value of integral width of (200) suggests that polar clusters have to be present.

A dielectric dispersion and a shift of $T_{\epsilon_{\max}}$ with increasing frequency towards higher temperatures is very distinct, but it is not similar to that observed for relaxors (Fig. 5). Usually, this kind of dispersion as in Fig. 5 is observed for single crystals with complex domain structure that strongly changes before transition point and in ceramics built of grains, and

boundaries between them. Looking at the dependence $\epsilon'(T)$ above $T_{\epsilon_{\max}}$, measured at 0.5 kHz, one cannot exclude the existence of a metal (electrode)-dielectric (surface) contact and the presence of electric conductivity that influences the total dielectric response. The comparison of zero-field and field cooling $\epsilon'(T)$ dependencies (the field strength of 0.5 kV/cm was applied at 300 °C) is another proof that the investigated ceramics is not a *classical* relaxor. These dependencies, for 5 kHz and 1 MHz frequencies, are presented in Fig. 6. The action of the d.c. electric field reduces values of ϵ' , changes the asymmetry of the $\epsilon'(T)$ runs around 200 °C, but does not induce any anomaly of $\epsilon'(T)$ at 152 °C, where distinct changes of piezoelectric properties have been detected. In our opinion, these results are a proof for polar micro/nano-regions existence far above 200 °C and their role in the appearance of dielectric dispersion, which is rather a relaxor-like than pure relaxor dispersion. A local stoichiometry in sample composition has been verified by means of ISM-5410 scanning electron microscope, with an energy dispersion X-ray spectrometer (EDS). Quantitative point microanalysis with the implementation of SEMQuant software elaborated by

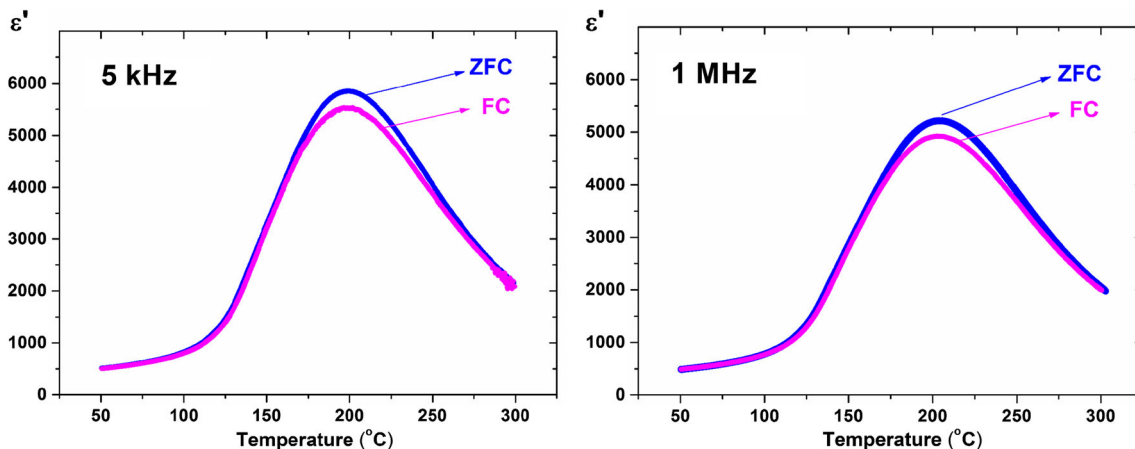
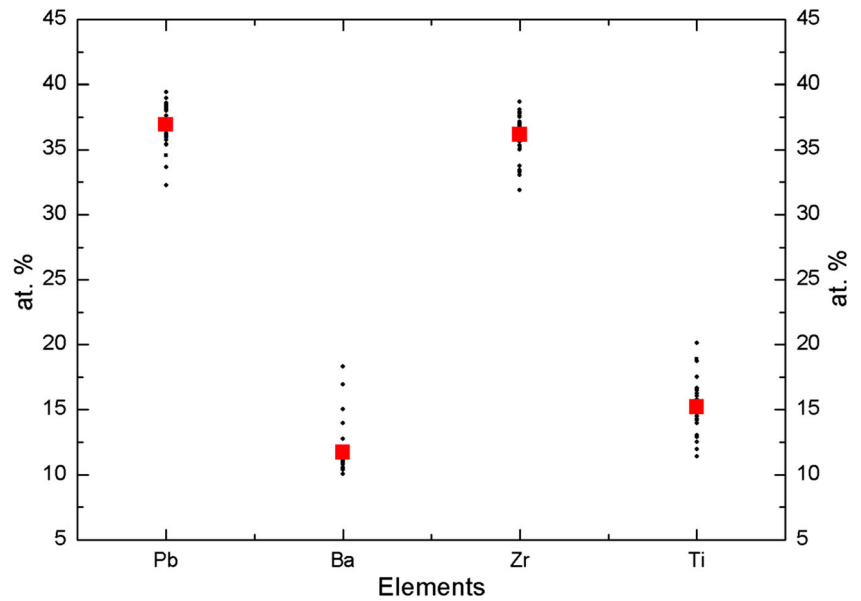


Fig. 6 Two dependencies, for zero-field cooling (ZFC) and field-cooling (FC), of permittivity versus temperature

Fig. 7 Real and average concentration of Ba, Pb, Zr and Ti ions measured for 25 points distributed on the surface of 10 randomly selected grains



Oxford Instruments (Link ‘ISIS’ Series System) was made, taking into account the radiation intensity from the excited Pb, Ba, Zr and Ti ions. Scanning was performed in 25 points of several grains for ceramics being subject of investigation. It was found that stoichiometry varies, and e.g. the amount of Pb ions varies from 32.3 at.% to 39.5 at.% (Fig. 7). Similar differences have been observed for Ba, Zr, and Ti ions. However, it should be emphasized that the average stoichiometry is in good agreement with the theoretical one. The measurement inaccuracy in the case of EDS microanalysis is at the level of 1% (Table 1). One can assume that the fluctuation in chemical composition of grains leads to a distribution of transition temperatures in the bulk of ceramics. Hence, it would be comprehensible why spontaneous polarization starts disappearing at temperatures significantly lower than $T_{\epsilon_{\max}}$. It would mean that after crossing $T_{\epsilon_{\max}}$, the remaining polar clusters are surrounded by a paraelectric cubic matrix. The depolarization field associated with polarization in these clusters would lead to locally compensated clusters structure (smaller clusters can have sizes of several hundred angstroms [17]). These clusters may thus be responsible for relaxor-like behaviour, in particular for the low frequency dielectric dispersion. On the other hand, such screening, by electrons or space charges, could cause huge thermal depolarization currents observed at temperatures considerably higher than $T_{\epsilon_{\max}}$ [14].

The elastic and piezoelectric properties seem to confirm the hypothesis of a special role of stable domains below $T_{\epsilon_{\max}}$ and clusters remaining above it. Temperature changes of the real and imaginary parts of elastic compliances are presented in Figs. 8 and 9. The value of elastic compliance at constant electric field s_{ij}^E and at constant electrical displacement s_{ij}^D is related to electromechanical coupling factor k_{ij} through the relation of $s_{ij}^D = s_{ij}^E(1 - k_{ij}^2)$ [20]. Starting from low

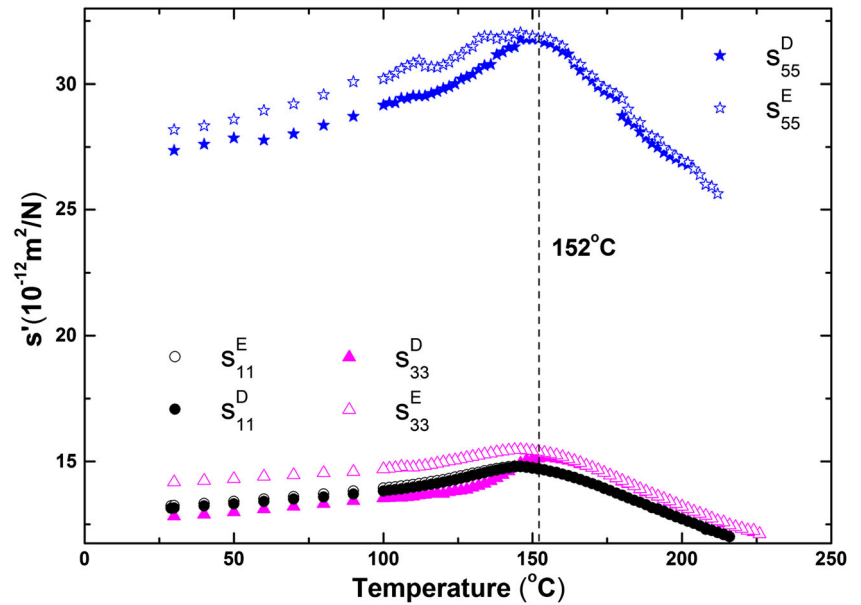
temperatures, the values gradually increase, eventually becoming of diffuse nature. The imaginary part of elastic compliances has a distinct maximum at 152 °C, which should be attributed to the absorption of the elastic energy due to internal frictions caused by piezoelectric vibrations. This temperature stays in good agreement with temperature where strong decrease of remnant polarization has been observed [14]. In particular, this absorption would be accountable for two mechanisms of clusters dynamics: the dipole flipping of clusters and movement (breathing) of polar cluster boundaries [21]. Below 152 °C the dynamics of polar clusters is absent (frozen), and the piezoelectric properties stabilize. On heating, those mechanisms lead to elastic lattice softening, manifesting a maximum of s' at 152 °C (Fig. 8).

It is worth noting that the difference between s_{ij}^E and s_{ij}^D is proportional to the product of the piezoelectric and dielectric properties $s_{ij}^E - s_{ij}^D = d_{mj}d_{nj}/\epsilon_{mn}$ [17, 22]. This difference (treated as the piezoelectric contribution to the compliance) is pronounced below 152 °C, when after poling in d.c. field the polar (ferroelectric-like) state with long-range interaction is stable. On the other hand, it is distinctly lesser above 152 °C, because of a disorder in clusters orientation, due to softening of lattice and de-freezing of clusters (Fig. 8).

Table 1 Nominal and average concentration of Ba, Pb, Zr and Ti ions

Ions	Nominal stoichiometry at %	Average content at %
Pb	37.5	36.9
Ba	12.5	11.7
Zr	35	36.1
Ti	15	15.2

Fig. 8 The real part of the elastic compliances s' as a function of temperature



In the cubic phase, the relation $s_{11} = s_{33}$ has to be fulfilled [22]. Yet, in the investigated ceramics these elastic compliances differ even above 200 °C (Fig. 8). It is in good agreement with the already mentioned results of X-ray diffraction and it confirms the existence of polar clusters (micro/nano-clusters) in the paraelectric cubic matrix. The interactions of these clusters through the cubic matrix result in the macroscopic piezoelectric response of the sample above 200 °C. When piezoelectric vibrations of clusters are too weak to overcome elastic stiffness of the matrix, the macroscopic piezoelectric deformation is no longer possible. It does not mean, however, that these polar clusters disappear completely. What can be said is that - for the investigated PBZT 25/70/30 ceramics - the macroscopic

piezoelectric resonances have not been registered above 220 °C (Figs. 10 and 11). The coefficients characterizing piezoelectric modulus are continuous function of temperature below 152 °C. Between 152 °C and 220 °C, the values of piezoelectric modulus vary in an irregular manner, and they are even unstable. It can also be accountable for the existence of unstable polar micro/nano-clusters.

4 Conclusions

The diffused temperature run of the permittivity can be explained by fluctuations in the chemical composition of PZT

Fig. 9 Temperature dependence of the imaginary part of the elastic compliances $s''_{11}^E, s''_{11}^D, s''_{33}^E$ and s''_{33}^D

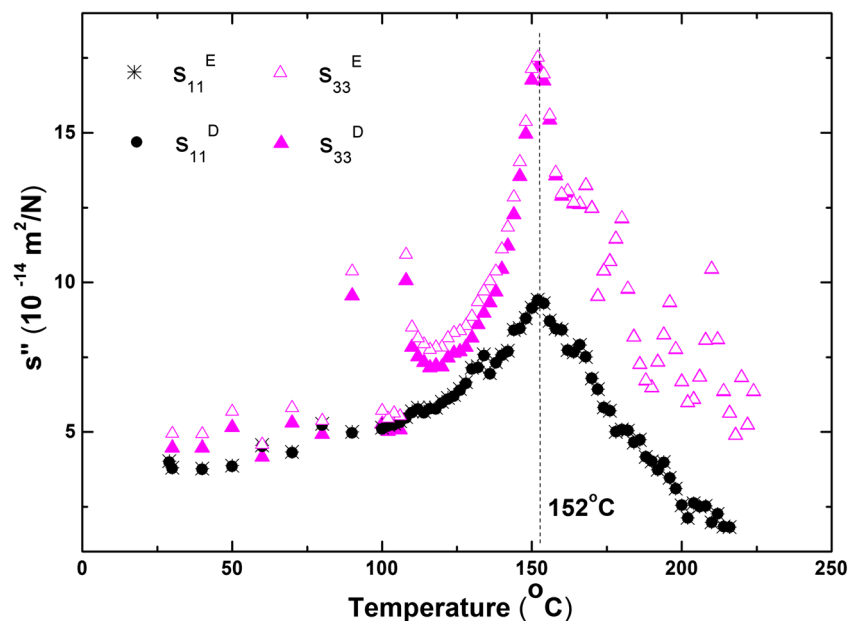
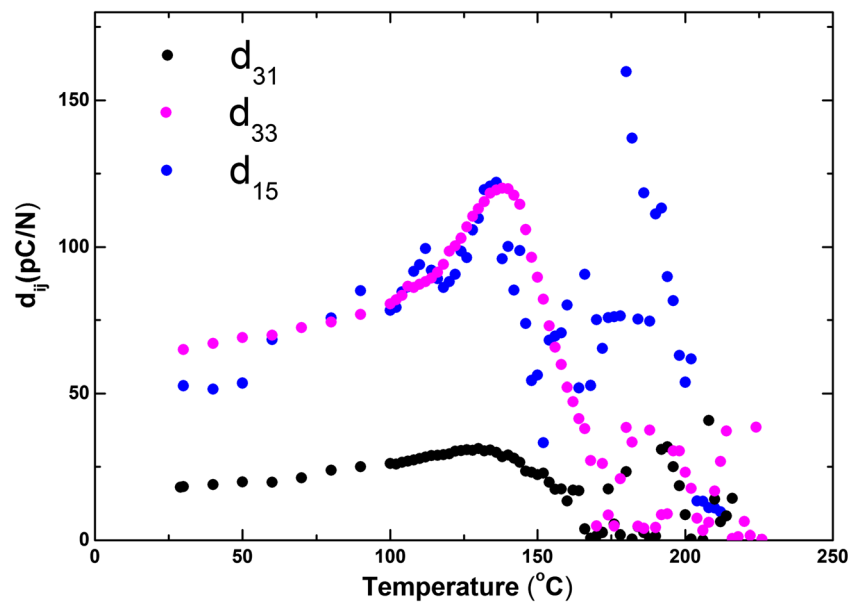


Fig. 10 The piezoelectric modulus d_{31} , d_{33} and d_{15} versus temperature determined for PBZT 25/70/30 ceramics



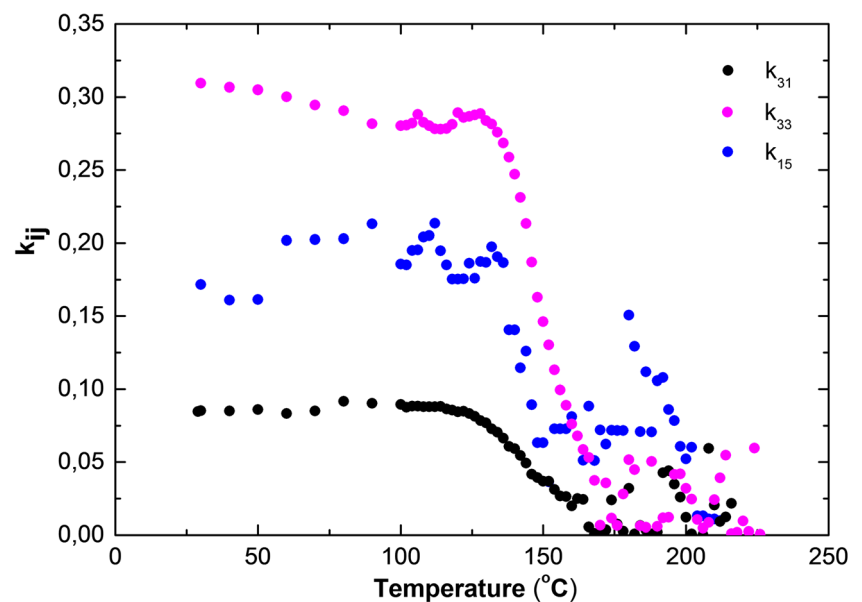
ceramics (Fig. 7) that lead to the broadening of the temperature range, in which the main transition between the paraelectric and ferroelectric phases appears. According to the phase diagram of pure PZT [20, 23], this main structural transition in the PZT70/30 ceramics occurs at around 340 °C. Thus, the variation of Zr content found in the investigated ceramics causes that this transition is realised between 290 °C (for 78% Zr) and 360 °C (for 64% Zr). Doping with Ba additionally lowers the value of these temperatures, as reported in [24, 25].

The difference between temperature points at which strong softening of the elastic properties takes place (152 °C) and piezoelectricity vanishes (220 °C) is equal to 68 °C, which

well corresponds to difference in T_c 's for PZT with fluctuations in Zr content, mentioned above.

The abnormally substantial integral width of the (200) reflection indicates the presence of a mixture of phases in the whole temperature range investigated. After poling in d.c. electric field, the lattice becomes averagely polar, of ferroelectric-like nature, and thus bulk piezoelectric properties can be observed. However, above the temperature of 152 °C long-range polar state decays and eventually polar micro/nano-clusters embedded in the cubic matrix appear. Random electric fields produced by these polar clusters can polarize the lattice in their neighbourhood, and thus make the volume of polar clusters fluctuate. That is why unstable piezoelectric

Fig. 11 Temperature dependence of the electromechanical coupling factors k_{31} , k_{33} and k_{15}



signals in the range between 152 °C and 220 °C have been detected. The interactions between polar regions through the paraelectric matrix finally vanish above 220 °C, but locally the symmetry can be broken (to become a polar one), even up to very high temperatures.

In typical relaxor there is a *critical* field above which additional phase transition is observed. We did not observe any transition induced by the d.c. electric field, although the applied electric field was stronger than the *critical* one mentioned above and equal to 1.5 kV/cm [26]. Based on properties described above, we claim that it is not allowed to label the investigated material a relaxor, although some similarities can be found [14]. We think that in the case of PBZT 25/70/30 ceramics the term relaxor-like material might be justified at most.

Acknowledgements The authors thank Irena Gruszka from the University of Silesia for technical assistance during sample preparation. We would like to acknowledge the late Michał Górný, who passed away in January 2016, for very fruitful cooperation.

This work was supported by the National Science Centre, Poland [grant number 2016/21/B/ST3/02242].

Open Access This article is distributed under the terms of the Creative Commons Attribution 4.0 International License (<http://creativecommons.org/licenses/by/4.0/>), which permits unrestricted use, distribution, and reproduction in any medium, provided you give appropriate credit to the original author(s) and the source, provide a link to the Creative Commons license, and indicate if changes were made.

References

1. K. Uchino, *Ferroelectric devices* (Marcel Dekker, New York, 2000)
2. Y. Xu, *Ferroelectrics Materials and their Applications* (Elsevier, The Netherlands, 1991), pp. 101–162
3. G.H. Heartling, C.E. Land, *J. Am. Ceram. Soc.* **54**, 1 (1971)
4. H. Kanai, O. Furukawa, H. Abe, Y. Yamashita, *J. Am. Ceram. Soc.* **77**, 2620 (1994)
5. G.A. Smolenskii, A.I. Agranovskaya, N. Krainik, *Dokl. Akad. Nauk SSSR* **91**, 55 (1953)
6. T. Ikeda, *J. Phys. Soc. Jpn.* **14**, 168 (1959)
7. G. Li, G. Haertling, *Ferroelectrics* **166**, 31 (1995)
8. L.E. Cross, *Ferroelectrics* **76**, 241 (1987)
9. A. Mesquita, A. Michalowicz, V.R. Mastelaro, *J. Alloys Compd.* **640**, 355 (2015)
10. F.S. Ahmed, K. Taibi, O. Bidault, N. Geoffroy, N. Millot, *J. Alloys Compd.* **693**, 245 (2017)
11. K. Ramam, M. Lopez, *J. Phys. D: Appl. Phys.* **39**, 4466 (2006)
12. A. Thongtha, C. Wattanawikkam, T. Bongkarn, *Phase Transit.* **84**, 952 (2011)
13. D. Bochenek, R. Skulski, P. Wawrzala, D. Brzezińska, *J. Alloys Compd.* **509**, 5356 (2011)
14. Z. Ujma, M. Adamczyk, J. Hańderek, *J. Europ. Cer. Soc.* **18**, 2201 (1998)
15. J. Hańderek, M. Adamczyk, Z. Ujma, *Ferroelectrics* **233**, 253 (1999)
16. K. Roleder, I. Franke, A.M. Glazer, P.A. Thomas, S. Miga, J. Suchanicz, *J. Phys. Condens. Matter* **14**, 5399 (2002)
17. I. Franke, K. Roleder, L. Mitoseriu, R. Piticescu, Z. Ujma, *Phys. Rev. B* **73**, 144114 (2006)
18. A. Bauer, D. Buhling, H.J. Gesemann, G. Helke, W. Schreckenbach, *Technology and Application of Ferroelectrics* (Akademische Verlagsgesellschaft Geest & Portig K.-G, Leipzig, 1976)
19. M. Mir, V.R. Mastelaro, P.P. Neves, A.C. Doriguetto, D. Garcia, M.H. Lente, J.A. Eiras, Y.P. Mascarenhas, *Acta Cryst. B* **63**, 713 (2007)
20. B. Jaffe, W.R. Cook, H. Jaffe, *Piezoelectric Ceramics* (Academic, London, 1971)
21. V. Bovtun, V.R. Porokhonsky, M. Savinonv, A. Pashkin, V. Zelezny, J. Petzelt, *J. Europ. Cer. Soc.* **24**, 1545 (2004)
22. J. F. Nye, *Physical Properties of Crystal* (Clarendon, Oxford, 2001)
23. N. Zhang, H. Yokota, A.M. Glazer, Z. Ren, D.A. Keen, D.S. Keeble, P.A. Thomas, Z.-G. Ye, *Nat. Commun.* **5**, 5231 (2014)
24. M. Adamczyk, Z. Ujma, L. Szymczak, A. Soszyński, *Ceram. Int.* **32**, 877 (2006)
25. Q. Tan, Z. Xu, J.-F. Li, D. Viehland, *J. Appl. Phys.* **80**, 5866 (1996)
26. N. Novak, R. Pirc, M. Wencka, Z. Kutnjak, *Phys. Rev. Lett.* **109**, 037601 (2012)